Title: Reactivating and reorganizing activity-silent working memory: two distinct mechanisms underlying pinging the brain

Abbreviated title: two distinct mechanisms of pinging the brain

Can Yang[1], Xianhui He[1], and Ying Cai[*1]

[1]Department of Psychology and Behavioral Sciences, Zhejiang University, Hangzhou, China, 310000

[*]Corresponding Author: yingcai@zju.edu.cn

Number of pages: 40

Number of figures: 6

Number of words: Abstract: 234; Introduction: 650; Discussion: 1530

Conflict of interest: The authors declare no competing financial interests.

Acknowledgments: This work was supported by the National Natural Science Foundation of China (32100851), the Zhejiang Provincial Natural Foundation Grant (LQ21C090005), the Fundamental Research Funds for the Central Universities (2021FZZX001-06), and the Research of Basic Discipline for the 2.0 Base of Top-notch Students Training Program, the Ministry of Education of China (20211033).

Abstract

Recent studies have proposed that visual information can be maintained in an activity-silent state during working memory (WM) and that this activity-silent WM can be reactivated by task-irrelevant high-contrast visual impulses (i.e., "pinging the brain"). Although pinging the brain has become a popular tool for exploring activity-silent WM in recent years, its underlying mechanisms remain unclear. In the current study, we directly compared the neural reactivation effects and behavioral consequences of context-independent and context-dependent pings to distinguish between the noise-reduction and target-interaction hypotheses of pinging the brain. In this electroencephalogram study, our neural decoding results showed that the context-independent pings reactivated activity-silent WM without changing the original representations of memorized items and that reactivation effects were significantly higher in individuals with poorer WM performance. In contrast, the context-dependent pings reactivated activity-silent WM in a more durable and consistent way and further reorganized it by decreasing the variability of items' neural representations and disturbing the memory structure between items. Notably, reactivation effects were stronger in the trials with larger recall errors. In an additional behavioral study, we optimized our experimental design to minimize expectation and adaptation effects and found that, compared with the baseline condition (no ping), context-dependent pings impaired recall performance, while context-independent pings did not. Together, our results provided clear evidence for two distinct mechanisms underlying pinging the brain, and the ping's context played a critical role in reactivating and reorganizing activity-silent WM.

Significance Statement

Working memory (WM) is the ability to temporarily maintain and manipulate information; notably, it can be maintained in an activity-silent state in which the information cannot be decoded. Such undecodable information can be reactivated by specific visual impulses (i.e., pings), providing direct evidence of activity-silent WM. In this study, we clarified two distinct mechanisms of pinging the brain: pings without contextual information related to the memorized items reactivated WM by reducing noise and did not change the original WM process, while pings with contextual information reactivated and reorganized WM, impairing memory performance. Our findings offer valuable insights for future studies utilizing pings as a research tool and contribute to our understanding of activity-silent WM.

Introduction

Working memory (WM) is the ability to temporarily maintain and manipulate information (Baddeley, 2003). An increasing number of studies have demonstrated that humans can prioritize WM information to guide behaviors (Gazzaley & Nobre, 2012; Myers et al., 2017). Earlier studies using multivariate pattern analyses showed that the neural representations of prioritized memory items (PMIs) were sustained during maintenance, while those of unprioritized memory items (UMIs) dropped to baseline but rebounded as needed (Lewis-Peacock et al., 2012; Sprague et al., 2016). A series of recent studies explored such WM processes by pinging the brain with task-irrelevant visual impulses (the "ping") and revealed some insightful but controversial results.

In a pioneering study, Wolff et al. (2015) found that the neural representation of a single item in WM returned to baseline during maintenance. Moreover, they proposed that this WM became activity-silent rather than disappearing, as a high-contrast white patch could reactivate the item's neural representation. Subsequent studies extended this finding to multi-item WM, revealing that both activity-silent PMIs and UMIs could be reactivated by pings (Wolff et al., 2017; Wolff et al., 2020b). Some computational models also supported the concept of activity-silent WM and suggested that it was achieved via transient changes between synapses instead of sustained neural firing (Barak & Tsodyks, 2014; Mongillo et al., 2008). However, such reactivations were not observed in some other studies, especially for UMIs, which suggested differences between PMI and UMI storage even though both were activity-silent (Fan & Luo, 2022; Huang et al., 2021). Currently, pinging the brain has become an important tool for investigating activity-silent WM, but the underlying mechanisms remain debated, thus limiting its usefulness.

Initially, pings were described as "sonar" that could reach the activity-silent memory within the brain network and generate a detectable echo (Wolff et al., 2015). However, a recent study found that pings reduced the across-trial variability of electroencephalograph (EEG) signals, suggesting that pings reactivate activity-silent representations by indirectly reducing overall neural noise (Barbosa et al., 2021; Fig. 1*A*; "noise-reduction hypothesis"). Alternatively, pings may directly strengthen activity-silent representations through shared context with WM items (Fig. 1*B*; "target-interaction hypothesis"). Supporting the target-interaction hypothesis, previous studies

have demonstrated that context information, such as location (Yu et al., 2020) and order (Huang et al., 2021), was automatically encoded and maintained alongside content information. These findings indicated that pings may indeed interact with memorized items through the shared context. However, direct evidence for the target-interaction hypothesis is lacking. Meanwhile, the key to distinguishing these two hypotheses is understanding how the context of pings affects reactivations. Unfortunately, most previous studies presented pings overlapping with item locations (Duncan et al., 2023; Kandemir et al., 2022; Wolff et al., 2017), making investigation of the functional role of the context of pings challenging.

In the current study, we directly compared neural reactivations from two types of pings: a "context-dependent ping" presented at a location overlapping with the position of the WM items and a "context-independent ping" presented at a different location to the WM items. Particularly, we tested some specific predictions of the noise-reduction and target-interaction hypotheses. First, the target-interaction hypothesis predicts the context-dependent pings would be more efficient in reactivating activity-silent WM due to the guidance of the common context (like a sonar system equipped with a sighting device), but the noise-reduction hypothesis does not make this prediction. Second, the target-interaction hypothesis predicts more consistent reactivations after multiple context-dependent pings, given that the context of items should be stable during WM maintenance (Cai. et al., 2020; Yu et al., 2020). In contrast, the noise-reduction hypothesis makes no such prediction since neural noise can be random and state-dependent. More importantly, the assumption that a context-dependent ping could reorganize the neural

representations of activity-silent WM or cause any behavioral consequence, which is compatible with the target-interaction hypothesis. In contrast, one of the most fundamental aspects of the noise-reduction hypothesis is that reactivations do not change the original WM process.

EEG Experiment

Materials and methods

Participants

Thirty-one right-handed volunteers (10 females, M_{age} = 22.5 years, SD_{age} = 3.03 years) participated in the EEG experiment and compensated for their participation (30 CNY/h). The sample size was determined based on previous studies (Wolff et al., 2017; Wolff, Kandemir, et al., 2020a). Informed written consent was obtained from each participant before the experiment, and ethical approval was obtained from the institutional review board of the Department of Psychology and Behavioral Sciences, Zhejiang University. Participants had normal or corrected-to-normal vision and no reported neurologic or psychiatric disease history.

Procedure

Participants completed an orientation delayed estimation task adapted from a previous study (Wolff et al., 2017; Fig. 2*A*). At the beginning of each trial, participants received instructions indicating the recall order for two orientations. Following a 1000 ms fixation period, two randomly oriented gratings appeared to the left and right (6° eccentricity from the centered fixation) for 250 ms. These gratings were sine-wave patterns with a contrast of 20%, a diameter

of 6°, and a spatial frequency of 0.65 cycles per degree. The orientations were selected randomly from a pool of 36 options, ranging from 0° to 180° in 5° increments; a minimum difference of 20° was ensured between any two orientations presented in the same trial. After a delay of 950 ms, the first ping was presented for 100 ms. Our task included two ping conditions. In the context-dependent ping condition, three white circle impulses (6° in diameter) were horizontally presented, with the left and right impulses completely overlapping with the locations of the memorized items during the sample period. In contrast, the context-independent ping condition involved the same three impulses but was rotated 90° from the context-dependent ping, and it did not overlap in location with the memorized items. The centered visual impulse was included to emphasize the task irrelevance of the pings. After another 500 ms delay, participants were required to recall the prioritized item by moving the mouse to select the corresponding orientation value, with a maximum response time of 4 seconds. The second ping appeared 800 ms after the first response. In each trial, the second ping was identical to the first ping. After an additional 400 ms delay, participants were tasked with recalling the unprioritized item in the same manner. Participants completed two separate sessions, each dedicated to one of the two ping conditions. The sessions were scheduled 48 hours apart, and the recall order remained consistent within each session. This design aimed to maximize the signal-to-noise ratio (SNR) for neural coding analyses (Wolff et al., 2017). The order of recalling two orientations and the order of two ping conditions were counterbalanced across participants. Each ping condition consisted of 540 trials across 9 blocks, and participants completed all the trials within approximately 90 minutes per day.

The experiment was programmed and executed using MATLAB (MathWorks) and the Psychophysics Toolbox extension (http://psychtoolbox.org). Visual stimuli were displayed on a 17-inch CRT monitor with a refresh rate of 100 Hz and a resolution of 1024 x 768 pixels. Participants were seated in a dark room and maintained a viewing distance of approximately 60 cm from the screen. The background color of the screen was set to gray (RGB = 128, 128, 128) throughout the experiment to minimize potential visual distractions.

EEG acquisition and preprocessing

During the experiment, EEG was recorded with a Biosemi Active Two recording system with a sampling rate of 1024 Hz. The 64 Ag/AgCl electrodes were positioned according to the extended 10–20 system, with a reference of a common mode sense electrode (CMS/DRL). During the recording, the impedances of all the channels were kept below 15 kΩ. EEG data preprocessing and analysis were conducted using the functions in the EEGLAB toolbox (Delorme & Makeig, 2004) and customized MATLAB scripts. Any horizontal eye movements were monitored by the horizontal electrooculogram (EOG) placed at the outer canthus of the two eyes, and vertical eye movements were monitored by the vertical EOG placed above and below the left eye. Raw EEG data were first downsampled to 256 Hz, bandpass filtered (0.1–40 Hz), and segmented into two epochs for each trial (from -2 s to 2 s relative to the onset of the first and second pings; we segmented the two epochs separately since the response time of the first recall was self-paced). After segmentation, bad EEG channels were identified by visual inspection and then interpolated

using the "spherical" method in EEGLAB. Baseline removal was conducted by subtracting the averaged activity during the 200 ms prestimulus interval. Eye blinks and muscle artifacts were identified through independent component analysis (ICA) and removed from the data. Finally, the post-ICA data were carefully visually inspected for any potential remaining artifacts, which were then rejected. As a result, 13.37% (SD = 5.46%) of the trials were excluded, and approximately 460 trials were kept for each ping condition (context-dependent ping: Mean ± SD = 465 ± 30.79; context-independent ping: Mean ± SD = 452 ± 47.17). One participant was excluded from all subsequent EEG analyses due to poor signal quality (more than 30% bad trials in both ping conditions).

Data analysis

Behavioral performance estimations

The response time (RT) was defined as the duration between the onset of the probe and mouse-click response, and the response error was calculated as the distance between the chosen value and the targeted value. To examine whether context-dependent and context-independent pings had different behavioral effects, paired t tests were conducted separately for RT and response error. All behavioral analyses were performed using customized MATLAB scripts and JASP (http://jasp-stats.org/). In two recalls, paired-sample t test results revealed no differences in recall error or RT between the two ping conditions ($ps > 0.273$, $BF_{10s} < 0.343$; Fig. 2*B*). In the following EEG analyses, all decoding analyses were conducted during the first 1 s after the response probe since the mean RTs were approximately 1 s in both recalls (recall 1: mean ± SD =

1.01 ± 0.48 s; recall 2: mean ± SD = 1.10 ± 0.51 s).

Estimation of the decoding strength of neural representations

We estimated the neural representations of PMIs and UMIs in each ping condition separately. For each time point, we extracted the voltage pattern across 17 parietal and occipital channels (P7, P5, P3, P1, Pz, P2, P4, P6, P8, PO7, PO3, POz, PO4, PO8, O1, Oz and O2), and we normalized these signals by subtracting their average value. Then, we aggregated the voltage patterns at 5 consecutive time points (including the time point of interest and the adjacent four time points) for neural decoding analyses. By taking both spatial and temporal information into consideration, more sensitive decoding of neural representations could be obtained (Fan & Luo, 2022; Wolff et al., 2020a). Additionally, the selected posterior electrodes were based on previous studies (Muhle-Karbe et al., 2021; Wolff et al., 2017). Next, we used the Mahalanobis distance method and the leave-one-trial-out cross-validation approach to estimate the decoding strength of neural representations across the trials (Wolff et al., 2017). For each trial, the data from that trial served as the testing data, and the data from all the remaining trials served as the training dataset. The training trials were divided into 12 bins based on their orientations relative to the test trial, the neural activity patterns of the trials labeling the same bin were averaged, and the Mahalanobis distances were calculated between the spatiotemporal neural activity pattern of the test trial and of each training bin. To estimate the decoding strength, 12 sign-reversed Mahalanobis distances were multiplied by the cosine of the center angle of each bin. This procedure was repeated for all trials and all time points, and the decoding strengths were averaged over trials, smoothed over

time with a Gaussian smoothing kernel (SD = 16 ms) and then averaged across participants. Finally, we utilized a nonparametric sign-permutation test to identify the time period in which the decoding strengths were significant (Maris & Oostenveld, 2007). For each time point, the sign of the decoding strength was randomly flipped for each participant, and the average was calculated. After 5,000 permutations, we obtained a null distribution of decoding strengths and obtained the threshold for significant decoding (with α set to 0.05, two-tailed). If two consecutive time points exceeded the threshold for significant decoding, we marked them as cluster candidates and aggregated their decoding strengths. Taking the decoding strengths of the 5,000 permutations for each time point together, we also obtained two null cluster-based distributions for the smallest and highest decoding strengths. *P* values referred to the proportion of the real cluster-based decoding strengths larger than the maximum null distribution or smaller than the minimum null distribution.

Some recent studies suggested that item-specific information could be sustainably decoded from posterior alpha power activities during WM maintenance and were not activity-silent (Barbosa et al., 2021; Foster et al., 2016). Thus, we also conducted a similar decoding analysis based on posterior alpha power activities (8~12 Hz) but did not observe reliable decoding results or any reactivation effects (see details in Fig. 3-1). Consequently, we focused on the decoding strengths from voltage signals in the following analyses.

Estimation of the reactivation strength after pings

To estimate the reactivation strength, we subtracted the post-ping decoding strengths (the averaged decoding strengths from 100~400 ms after the ping) from the pre-ping decoding strengths (the averaged decoding strengths from -100~0 ms before the ping). This subtraction was performed to capture the change in decoding strength specifically attributed to the ping stimulus and exclude any sustained decoding effects. The chosen post-ping time window was based on a previous study (Muhle-Karbe et al., 2021). Then, we used a bootstrapping procedure to examine whether the reactivation strengths for the PMIs and UMIs were significant in each ping condition. Specifically, we randomly resampled all the participants with replacement 5,000 times to obtain a null distribution of reactivation strengths for each ping condition, and the *p* values referred to the proportion of the null distribution less than the real reactivation strength. Moreover, we conducted a whole-brain searchlight analysis to identify the electrodes that contributed to neural reactivation. For each time point in each channel, we extracted the voltage signals from the two closest channels and four adjacent time points to represent the spatiotemporal pattern of the central channel. The decoding strengths and reactivation effects were estimated by a Mahalanobis distance method and leave-one-trial-out cross-validation approach similar to that mentioned above, and the statistical significance of electrode clusters was identified by a similar nonparametric sign-permutation test with 5,000 permutations.

To compare the reactivation strengths between the two ping conditions, we subtracted the reactivation strength in the context-independent ping condition from that in the context-dependent ping condition for each participant and conducted a similar bootstrapping procedure to

identify its statistical significance. This comparison was conducted for the first and second pings separately. Moreover, to investigate whether the context-dependent ping evoked more consistent reactivations between the first and second pings than the context-independent ping, we computed the Pearson correlation coefficient between each pair of reactivation effects for PMIs within a trial in the two ping conditions separately, and then we used a two-tailed z test to determine the statistical significance of the difference in the reactivation consistency between the two ping conditions.

Estimation of the behavioral correlates of the reactivation strengths

We focused our analyses on the first ping period when the PMI and UMI were simultaneously maintained and task-relevant (during the second ping period, PMIs became task-irrelevant items and UMIs became task-relevant items). To test the relationship between reactivation strengths and behavioral performance (recall error and RT), we conducted both trial-level and participant-level analyses. At the trial level, we divided all trials into two subgroups based on the median of the recall errors for the first recall for each participant; at the participant level, we divided all participants into two subgroups depending on the median of the averaged recall errors for the first recall among all participants. Then, we compared the reactivation strengths between the two subgroups at the trial level and participant level separately using bootstrapping procedures similar to those described above.

Estimation of the dynamic changes in neural representations after pings

We performed two series of analyses to examine the effects of context-dependent and context-independent pings on the dynamic changes in neural representations. First, we conducted cross-time decoding analyses to examine whether the context-dependent and context-independent pings differently affected the dynamics of activity-silent WM storage. We used a similar Mahalanobis distance method and the leave-one-trial-out cross-validation approach to estimate the decoding accuracy, except that we calculated the Mahalanobis distances between the spatiotemporal neural activity patterns across different time points. The decoding was performed separately for PMIs and UMIs in both context-dependent and context-independent ping conditions, and we generated difference matrixes by subtracting the decoding results between the two ping conditions. To assess the significance of the cross-time decoding strengths and the differences between the two ping conditions, we performed the same nonparametric sign-permutation test (with 5,000 permutations). *P* values were calculated as the proportion of the real cluster-based decoding strengths larger than the maximum null distribution cutoff or smaller than the minimum null distribution cutoff. Next, we focused on the time window after pings and quantified the dynamic changes in neural representations by three indices: the stable, generalized, and dynamic indices (Oh et al., 2019). The stable index represented the proportion of off-diagonal decoding strengths (trained and tested at different time points) that were significantly greater than zero but not significantly smaller than the corresponding on-diagonal strengths (trained and tested at the same time point). A higher stable index indicated greater stability of neural representations. The generalized index represented the proportion of off-diagonal decoding strengths that were significantly smaller than the corresponding on-diagonal

ones but simultaneously significantly greater than zero. A higher generalized index indicated slowly changing neural representations. The dynamic index represented the proportion of off-diagonal decoding strengths that were significantly smaller than the corresponding on-diagonal ones and not significantly greater than zero. A higher dynamic index indicated quickly changing neural representations. For each index and each time point, we performed a permutation test to determine the statistical significance of the difference between the two ping conditions. That is, we randomly permuted the labels of the ping conditions for each participant and calculated the differences of these three indexes, and we obtained a null distribution of the differences for each index through 5,000 permutations. The *p* values indicated the proportion of the null distribution that was less than the real index.

Second, we conducted cross-item decoding analyses to further examine whether the two types of pings affected the overall WM representational structure differently, as previous studies have found that PMIs and UMIs are coded in a suppressive pattern (van Loon et al., 2018; Yu et al., 2020). Similarly, we estimated the decoding strengths using Mahalanobis distances, this time between neural patterns of PMIs and UMIs (i.e., trained on PMI and tested on UMI). We subtracted the post-ping decoding strengths (averaged decoding strengths from 100~400 ms after the ping) from the pre-ping decoding strengths (averaged decoding strengths from -100~0 ms before the ping), and we used the same bootstrapping procedure to estimate the significance of reactivation effects of the memory structure in two ping conditions as well as their differences.

EEG results

Context-dependent pings evoked more sustained reactivation for prioritized items than context-independent pings

In the context-independent ping condition, both PMIs and UMIs could be decoded during the sample and early delay period, while the decoding strengths decayed to baseline during the maintenance period (relative to the onset of the sample, PMI decoding: from 74 ms to 840 ms; UMI decoding: from 82 ms to 453 ms), suggesting that both PMIs and UMIs were maintained in an activity-silent state. Then, only the neural representations of PMIs rebounded after the ping (relative to the onset of the first ping, from 113 ms to 536 ms) and were maintained until the early first recall (relative to the onset of the probe display, from 78 ms to 551 ms). Consistently, during the second ping period, only the decoding for task-relevant items rebounded after the ping and was sustained until the second recall period (relative to the onset of the second ping, from 101 ms to 1451 ms; Fig. 3*A*, first row). In the context-dependent ping condition, the decoding results were quite similar to those in the context-independent condition before the first ping. However, the rebound of PMI representation was sustained longer after the first ping; the decoding strengths were significant during the whole first recall period (relative to the onset of the first ping, from 63 ms to 1600 ms) and the early second ping period (relative to the onset of the second ping, from -500 ms to 364 ms). In contrast, there was no reactivation observed for task-relevant items after the second ping in the context-dependent condition (Fig. 3*A*, second row).

Furthermore, we directly compared the immediate reactivation strengths between the context-dependent ping and context-independent ping conditions. Our results showed that there was no difference between the two conditions after the first ping ($p = 0.206$), but the context-independent ping evoked a greater reactivation for task-relevant items than the second ping in the context-dependent ping condition ($p = 0.025$; Fig. 3*B*). To further compare the sustained reactivation strengths of the first ping between the two ping conditions, we compared the decoding strengths before the onset of the second ping in the two ping conditions (-100~0 ms before the second ping). Our results showed that the decoding strengths for both items were significant in the context-dependent ping condition ($ps < 0.009$), while neither was significant in the context-independent ping condition ($ps > 0.231$). The decoding strengths for first-recall items in the context-dependent ping condition were significantly larger than those in the context-independent ping condition ($p = 0.009$), and the same pattern of differences were also marginally significant for the second-recall items ($p = 0.067$; Fig. 3*C*). These results suggested that although comparable immediate reactivation strengths were observed in both ping conditions, context-dependent ping affected neural representations of both items more durably.

In addition, whole-brain searchlight results suggested that these significant neural reactivation effects were mainly contributed to the posterior parietal-occipital electrodes (Fig. 3*A*). To better demonstrate the decoding results in other brain areas, we performed parallel reactivation strength analyses among 17 anterior and mid-central electrodes but did not observe any neural reactivation effects in either ping condition (see more details in Fig. 3-2). Therefore, we focused

all the following analyses on the neural representations among posterior channels.

Context-dependent pings evoked more consistent reactivation effects for prioritized items

Correlation analysis revealed that the context-dependent ping evoked highly consistent reactivation effects for PMIs after the first and second pings ($r = 0.728$, $p < 0.001$, $BF_{10} > 1000$). In contrast, there was no correlation between the first and second reactivations in the context-independent ping condition ($r = -0.17$, $p = 0.341$, $BF_{10} = 0.334$). The correlation difference between the two ping conditions was significant ($z = 3.779$, $p < 0.001$; Fig. 3*D*), suggesting that reactivation effects in the context-dependent ping condition were more consistent than those in the context-independent ping condition.

Reactivations after context-dependent and context-independent pings correlated with trial-level and participant-level recall performance separately

In the context-dependent ping condition, our subgroup comparisons revealed significantly weaker neural reactivation in the trials with larger recall errors than in the trials with smaller recall errors ($p = 0.007$), but no such difference was found between trials with different magnitudes of recall errors in the context-independent ping condition ($p = 0.152$; Fig. 4*A*, left). In contrast, in the context-independent ping condition, we observed significantly weaker reactivations for the participants with better recall performance than those with worse recall performance ($p = 0.014$), while no such difference was found in the context-dependent ping condition ($p = 0.133$; Fig. 4*A,* right). We also performed similar subgroup comparisons to

examine the relationship between neural reactivations and RTs at both the trial and participant levels, but similar differences were not observed in either ping condition (Fig. 4*B*).

Context-dependent ping stabilized the neural representations of prioritized items

The cross-time decoding results revealed that neural representations of both PMIs and UMIs were highly dynamic during the sample and maintenance periods, and there were no differences between the two ping conditions. However, the cross-time decoding strengths were higher after context-dependent pings than after context-independent pings (Fig. 5*A*). Consistently, the stable index and the generalized index were significantly higher after context-dependent pings than after context-independent pings, i.e., during the delay period after the ping and the whole first recall period; meanwhile, the dynamic index was higher in the context-independent ping condition (Fig. 5*B*). These results suggested that compared with the context-independent ping, the context-dependent ping reorganized the neural representations of the PMI by enhancing the stability of the neural representations.

Context-dependent ping changed the suppressive coding between PMIs and UMIs

In both ping conditions, the cross-item decoding analyses demonstrated that PMIs and UMIs were coded in a suppressive manner during the sample and early delay periods, while this suppressive coding pattern could not be detected in the later delay period (context-independent ping: from 78 ms to 1041 ms; context-dependent ping: from 101 ms to 710 ms; relative to the onset of the sample). Interestingly, suppressive coding was observed only after the context-

independent ping (from 98 ms to 930 ms, relative to the onset of the first ping) but not after the context-dependent ping (Fig. 5*C*), and the difference in the reactivations of the coding structure between the two ping conditions was significant (context-independent ping: $p = 0.003$; context-dependent ping: $p = 0.276$; ping difference: $p = 0.043$; Fig. 5*D*). Similarly, the cross-item decoding comparison (a.k.a. trained on UMIs and tested on PMIs) revealed comparable results (see more details in Fig. 5-1). These results suggested that the context-dependent ping changed the overall neural representation structure of activity-silent WMs, while the context-independent ping did not.

Behavioral Experiment

Our EEG study revealed that although both context-dependent and context-independent pings reactivated the neural representations of prioritized items, the context-dependent ping evoked a more durable reactivation and changed the dynamics of neural representations. However, we did not observe any behavioral differences between these two ping conditions. One possible explanation could be the potentially confounding influences of the expectation and adaptation effects, as the experiments for the two ping conditions were completed on separate days (for increasing the SNR for neural decoding). To address this limitation, we performed an additional behavioral study in which we used a retro-cue paradigm and interleaved the two ping conditions. In addition, to further examine the durability of ping effects, we only included one ping in the behavioral experiment.

Materials and Methods

Participants

Sixty right-handed volunteers (33 females; $Mean_{age}$ = 21.17 years, SD_{age} = 2.49 years) participated in the behavioral experiment and received compensation for their participation (30 CNY/h). The sample size was estimated using G*power 3.1 from a pilot experiment (with α set to 0.05; power set to 0.8). Informed written consent was obtained from each participant before the experiment, and ethical approval was obtained from the institutional review board of the Department of Psychology and Behavioral Sciences, Zhejiang University. Participants had normal or corrected-to-normal vision and no reported neurologic or psychiatric disease history.

Procedure

Participants completed a similar delayed estimation task as in the EEG experiment except the recall order was determined by two retro-cues in each trial, and only one ping was presented before the first recall (Fig. 6*A*). In each trial, the first cue appeared after the sample to indicate the item to be recalled, and the second cue appeared after the first recall and had a 50% probability of switching. In the switch condition, the item to be recalled second was the unprioritized item in the first recall (UMI); in the stay condition, the item to be recalled second was the same as the prioritized item in the first recall (PMI). Pings were presented after the first cue and before the first recall. Our task included three ping conditions: the context-dependent ping condition, the context-independent ping condition, and a baseline condition without any ping (a fixation dot was presented at the center of the screen). Each condition consisted of 104

trials divided into two blocks. The order of the blocks was pseudorandomized across participants, with the restriction that the adjacent two blocks corresponded to different ping conditions.

Data analysis

We estimated and analyzed the RT and response error in a similar manner as in our EEG experiment. Five participants were excluded due to poor behavioral performance (RT or recall error was more than 3 SDs away from the group means). For the responses during the first recall, we conducted one-way repeated-measures ANOVAs separately for RT and recall error to examine whether the three ping conditions led to different behavioral consequences. If the main effect was significant, we conducted further post hoc tests to determine the significance of the differences between the context-dependent ping and the baseline condition, as well as between the context-independent ping and the baseline condition. For the responses during the second recall, we first conducted a two-way repeated-measures ANOVA, with the within-participant factors of ping condition (context-dependent ping/context-independent ping/baseline) and item type (PMI/UMI). If the interaction effect was significant, we further conducted one-way repeated-measures ANOVAs and post hoc tests for PMI and UMI recall separately to check the differences between the three ping conditions. All reported *p* values were Holm–Bonferroni multicomparison corrected.

Results

For the response errors in the first recall, the one-way repeated-measures ANOVA revealed a

main effect of ping conditions ($F_{(2,108)} = 3.981$, $p = 0.021$, $BF_{10} = 1.698$; Fig. 6*B*, left). Post hoc tests demonstrated that the response error in the context-dependent ping condition was marginally larger than that in the baseline condition ($t_{(54)\,holm} = 2.041$, $p = 0.087$, $BF_{10} = 1.178$), but there was no difference between the context-independent ping condition and the baseline condition ($t_{(54)holm} = 0.667$, $p = 0.506$, $BF_{10} = 0.183$). The difference between the context-independent ping and the context-dependent ping was significant ($t_{(54)\,holm} = 2.708$, $p = 0.024$, $BF_{10} = 2.883$). For the response errors in the second recall, the two-way repeated-measures ANOVA results revealed a significant interaction effect between item type and ping condition ($F_{(2,108)} = 6.636$, $p = 0.002$, $BF_{10} = 17.754$). Further one-way repeated-measures ANOVA results showed a main effect of ping condition for PMI recall ($F_{(2,108)} = 6.391$, $p = 0.002$, $BF_{10} = 12.135$) but not for UMI recall ($F_{(2,108)} = 0.675$, $p = 0.511$, $BF_{10} = 0.108$; Fig. 6*B*, right). Post hoc tests showed that the response error for PMI in the context-dependent ping condition was larger than that in the baseline condition and the context-independent condition ($ts > 2.415$, $ps < 0.035$, BFs > 2.429), but there was no difference between the context-independent ping condition and the baseline condition ($t_{(54)\,holm} = 1.075$, $p = 0.285$, $BF_{10} = 0.284$). These results suggested that the context-dependent ping impaired the recall performance of prioritized items, and this ping effect lasted until the second recall. However, there were no RT differences among the three conditions in either recall for PMI or UMI ($Fs < 0.458$, $ps > 0.634$, BFs < 0.090).

Discussion

Our study demonstrated that context-dependent and context-independent pings reactivated

activity-silent WMs through distinct mechanisms. The context-independent ping reactivated the neural representations without changing the original WM process or impacting recall performance. In contrast, the context-dependent ping reactivated the activity-silent WM more durably and consistently and further reduced the neural representations' dynamism, leading to impaired recall performance. These findings highlighted the significance of shared context between items and pings for interacting with activity-silent WMs.

Our results suggested that a context-independent ping that did not overlap with the locations of memorized items could reactivate the activity-silent WM, supporting the noise-reduction hypothesis (Barbosa et al., 2021). Comparing previous studies that used pings that either totally or partially overlapped with memorized items' locations (Kandemir et al., 2022; Wolff et al., 2017), our results clearly demonstrated that the ping itself can reactivate activity-silent WM without relying on contextual information. Furthermore, our cross-time decoding results revealed highly dynamic neural representations after the presentation of a context-independent ping, consistent with previous studies (Ju & Bassett, 2020; Meyers et al., 2008; Spaak et al., 2017). Meanwhile, our cross-item decoding results showed that the suppressive coding pattern between the prioritized and unprioritized items was preserved after the context-independent ping. This suppressive coding pattern has been reported in a series of EEG (Wan et al., 2020), fMRI (van Loon et al., 2018; Yu et al., 2020), and computational modeling studies (Stokes et al., 2020; Wan et al., 2022), and researchers proposed that such a coding scheme could be more efficient in maintaining items in different WM states. Our results demonstrated that the context-independent

ping did not alter the dynamics of each activity-silent WM representation or their overall format. Additionally, we observed that individuals with lower baseline WM performance exhibited stronger reactivations after the context-independent ping. This suggested that individuals with poorer WM may have a noisier WM storage network, resulting in a lower threshold for items to become activity-silent and to be reactivated more easily. In contrast, we did not observe reactivation differences between better and worse recall trials, and our behavioral data showed no overall changes after context-independent ping. Therefore, our results suggested that the activity-silent threshold reflected individual trait differences rather than trial-level states.

Our results also provided evidence for the target-interaction hypothesis of pinging the brain. First, we found that compared with context-independent pings, context-dependent pings reactivated WM representations more durably and consistently, highlighting the direct pathway of pinging the brain through shared contextual information. These results were supported by some recent studies that also emphasized the importance of the contextual information of pings. For example, the critical role of sequence context in pinging was highlighted as only pings containing sequence information reactivated the ordinal position during WM (Fan & Luo, 2022), and in a visual search task, only pings at overlapping locations with a high probability of being tested reactivated item neural representations (Duncan et al., 2023). Second, we observed that context-dependent pings induced a reorganization of neural representations by reducing their variability. Specifically, there were significant commonalities in neural representations during the delay period after context-dependent pings and during recall, indicating the facilitation of neural

representation transformation from WM maintenance to response preparation. Recent studies have shown that individuals actively generate item-specific action plans and represent them in conjunction with WM content during the late delay period, resulting in faster behavioral responses (van Ede et al., 2019). This prospective action planning can even occur at the early visual input stage when the mapping between items and actions is fixed (Boettcher et al., 2021). However, we did not find a correlation between such neural representation transformations and response times at either the participant or trial level. In contrast, our results suggested that the original dynamic changes in neural representations may have a positive effect on recall performance, as the context-dependent ping led to overall worse recall performance, and trials with stronger reactivations after context-dependent ping were associated with worse recall performance. Consistent with these results, some intracranial EEG studies employing deep learning and pattern similarity analyses have demonstrated that highly dynamic neural representations during WM facilitate the transformation from maintaining visual details to abstract information, ultimately benefiting WM maintenance and long-term memory (Liu et al., 2020, 2021). However, some studies found that trials with stronger neural representations after ping were accompanied by higher recognition accuracy (Wolff et al., 2017), and others found no behavioral relevance of item-specific reactivations (Fan & Luo, 2022). We suggest that these inconsistent behavioral findings may arise from different experimental settings. In our EEG experiment, similar to most EEG studies, we used pre-sample cues and presented trials in blocks with the same recall order to maximize SNR for neural decoding and did not observe behavioral changes in either ping condition. In contrast, in our behavioral experiment, which minimized

confounding factors such as expectation and adaptation effects by using retro-cues and a mixed design, we observed worse recall performance specifically after context-dependent pings. These results suggest that precise experimental design is critical for answering specific research questions.

Furthermore, our results clarified several conflicts in the understanding of the activity-silent WM storage. One is that our results localized the activity-silent WM representations in the relevant sensory cortices. These results were consistent with previous studies reporting neural reactivations in the posterior electrodes (Kandemir et al., 2022; Wolff et al., 2017) and help to reconcile conflicting results that signals were measured by different electrodes (Schneegans & Bays, 2017; Trübutschek et al., 2019). Our results suggest that neural coding results using whole-brain signals should be interpreted with caution (Fan & Luo, 2022; Wolff et al., 2020b). The uniqueness of reactivation effects in the sensory cortex aligned with some previous studies. For instance, the sensory-recruitment theory of visual working memory (VWM) posited the critical role of the sensory cortices in maintaining item-specific WM information (Gayet et al., 2018; Harrison & Tong, 2009; Katus et al., 2015), and some recent studies have proposed that these representations were susceptible to external visual input during maintenance (Bettencourt & Xu, 2016).

Another noteworthy finding is that neither context-dependent nor context-independent pings reactivated the unprioritized items, implying that while both prioritized and unprioritized items

were undecodable in the activity-silent state, task priority also modulated WM states. These results were consistent with previous studies that have reported weaker reactivations for unprioritized items (Huang et al., 2021; Wolff et al., 2017) and that the unprioritized items are more resistant to external interruptions during maintenance (Zhang et al., 2022). In addition, a recent study suggested that WM items are reorganized into different activity-silent states depending on their sequence context and can be reactivated at different latencies during retention after pings (Huang et al., 2021). However, other studies found that unprioritized items can also be reactivated by pinging the brain (Huang et al., 2021; Wolff et al., 2017) or by transcranial magnetic stimulation (TMS) (Rose et al., 2016). We propose that these inconsistencies are due to various parameters of the pings used across studies. For example, pings can be high-contrast or pure white impulses (Wolff et al., 2015, 2017), be a single large visual stimulus covering almost the whole screen (Fan & Luo, 2022; Huang et al., 2021) or consist of several small visual patches wholly or partially covering the memorized items' locations (Duncan et al., 2023; Kandemir et al., 2022), and the duration of pings can also differ from 100 ms (Wolff et al., 2017) to 200 ms (Duncan et al., 2023). Thus, the efficiency of pings was a salient confounding factor and should be considered in future studies. Furthermore, the discrepancy between our findings and those of the TMS study may indicate that pinging and TMS operate through distinct mechanisms, and other investigations can explore these differences in future studies.

Although our study has provided valuable insights into the underlying mechanisms of pinging the brain, several important questions remain unanswered. First, although our results suggested

that the reactivation strengths after context-dependent and context-independent pings were not correlated, future studies are needed to determine whether these two mechanisms act independently or whether the reactivation effect of context-dependent pings is a combined result of both mechanisms. Second, our EEG results provided evidence for reactivations among the posterior electrodes while sustaining neural representations in frontal areas; future studies can use imaging techniques with both high temporal and high spatial resolution (such as magnetoencephalography) to further explore how pings affect the dynamics of neural representations across the whole brain. Additionally, to directly verify the neural dynamic changes after pings, it would be helpful to include a condition without pings and conduct cross-condition decoding analyses in future studies.

In summary, the current study directly compared neural reactivations and behavioral changes after context-independent and context-dependent pings. Our results clarified two distinct underlying mechanisms of pinging the brain: the context-independent ping reduces the sensory-network representation noise and evoked a neural echo without changing the original WM maintenance or behavioral performance, whereas the context-dependent ping accesses and interacts with activity-silent WM through an internal priority map that is organized by contextual information, resulting in impaired WM performance. These results offer valuable insights for future studies employing pings as a tool to investigate activity-silent WM and enhance our understanding of the activity-silent WM process.

References

Baddeley, A. (2003). Working memory: Looking back and looking forward. Nature Reviews Neuroscience, 4(10), 829–839. https://doi.org/10.1038/nrn1201

Barak, O., & Tsodyks, M. (2014). Working models of working memory. Current Opinion in Neurobiology, 25, 20–24. https://doi.org/10.1016/j.conb.2013.10.008

Barbosa, J., Lozano-Soldevilla, D., & Compte, A. (2021). Pinging the brain with visual impulses reveals electrically active, not activity-silent, working memories. PLOS Biology, 19(10), e3001436. https://doi.org/10.1371/journal.pbio.3001436

Bettencourt, K. C., & Xu, Y. (2016). Decoding the content of visual short-term memory under distraction in occipital and parietal areas. Nature Neuroscience, 19(1), Article 1. https://doi.org/10.1038/nn.4174

Boettcher, S. E. P., Gresch, D., Nobre, A. C., & Van Ede, F. (2021). Output planning at the input stage in visual working memory. Science Advances, 7(13), eabe8212. https://doi.org/10.1126/sciadv.abe8212

Cai, Y., Fulvio, J. M., Yu, Q., Sheldon, A. D., & Postle, B. R. (2020). The Role of Location-Context Binding in Nonspatial Visual Working Memory. Eneuro, 7(6), ENEURO.0430-20.2020. https://doi.org/10.1523/ENEURO.0430-20.2020

Delorme, A., & Makeig, S. (2004). EEGLAB: An open source toolbox for analysis of single-trial EEG dynamics including independent component analysis. Journal of Neuroscience Methods, 134(1), 9–21. https://doi.org/10.1016/j.jneumeth.2003.10.009

Duncan, D., Van Moorselaar, D., & Theeuwes, J. (2022). Pinging the brain to reveal the hidden

attentional priority map using encephalography [Preprint]. Neuroscience. https://doi.org/10.1101/2022.08.23.504931

Fan, Y., & Luo, H. (2023). Reactivating ordinal position information from auditory sequence memory in human brains. Cerebral Cortex, 33(10), 5924–5936. https://doi.org/10.1093/cercor/bhac471

Foster, J. J., Bsales, E. M., Jaffe, R. J., & Awh, E. (2017). Alpha-Band Activity Reveals Spontaneous Representations of Spatial Position in Visual Working Memory. Current Biology, 27(20), 3216-3223.e6. https://doi.org/10.1016/j.cub.2017.09.031

Foster, J. J., Sutterer, D. W., Serences, J. T., Vogel, E. K., & Awh, E. (2016). The topography of alpha-band activity tracks the content of spatial working memory. Journal of Neurophysiology, 115(1), 168–177. https://doi.org/10.1152/jn.00860.2015

Gayet, S., Paffen, C. L. E., & Van Der Stigchel, S. (2018). Visual Working Memory Storage Recruits Sensory Processing Areas. Trends in Cognitive Sciences, 22(3), 189–190. https://doi.org/10.1016/j.tics.2017.09.011

Gazzaley, A., & Nobre, A. C. (2012). Top-down modulation: Bridging selective attention and working memory. Trends in Cognitive Sciences, 16(2), 129–135. https://doi.org/10.1016/j.tics.2011.11.014

Harrison, S. A., & Tong, F. (2009). Decoding reveals the contents of visual working memory in early visual areas. Nature, 458(7238), 632–635. https://doi.org/10.1038/nature07832

Huang, Q., Zhang, H., & Luo, H. (2021). Sequence structure organizes items in varied latent states of working memory neural network. ELife, 10, e67589.

https://doi.org/10.7554/eLife.67589

Ju, H., & Bassett, D. S. (2020). Dynamic representations in networked neural systems. Nature Neuroscience, 23(8), 908–917. https://doi.org/10.1038/s41593-020-0653-3

Kandemir, G., Wolff, M. J., Karabay, A., Stokes, M. G., Axmacher, N., & Akyürek, E. G. (2022). Concurrent maintenance of both veridical and transformed working memory representations [Preprint]. Neuroscience. https://doi.org/10.1101/2022.10.28.514218

Katus, T., Grubert, A., & Eimer, M. (2015). Electrophysiological Evidence for a Sensory Recruitment Model of Somatosensory Working Memory. Cerebral Cortex, 25(12), 4697–4703. https://doi.org/10.1093/cercor/bhu153

Lewis-Peacock, J. A., Drysdale, A. T., Oberauer, K., & Postle, B. R. (2012). Neural Evidence for a Distinction between Short-term Memory and the Focus of Attention. Journal of Cognitive Neuroscience, 24(1), 61–79. https://doi.org/10.1162/jocn_a_00140

Liu, J., Zhang, H., Yu, T., Ni, D., Ren, L., Yang, Q., Lu, B., Wang, D., Heinen, R., Axmacher, N., & Xue, G. (2020). Stable maintenance of multiple representational formats in human visual short-term memory. Proceedings of the National Academy of Sciences, 117(51), 32329–32339. https://doi.org/10.1073/pnas.2006752117

Liu, J., Zhang, H., Yu, T., Ren, L., Ni, D., Yang, Q., Lu, B., Zhang, L., Axmacher, N., & Xue, G. (n.d.). Transformative neural representations support long-term episodic memory. Science Advances, 7(41), eabg9715. https://doi.org/10.1126/sciadv.abg9715

Maris, E., & Oostenveld, R. (2007). Nonparametric statistical testing of EEG- and MEG-data. Journal of Neuroscience Methods, 164(1), 177–190.

https://doi.org/10.1016/j.jneumeth.2007.03.024

Meyers, E. M., Freedman, D. J., Kreiman, G., Miller, E. K., & Poggio, T. (2008). Dynamic Population Coding of Category Information in Inferior Temporal and Prefrontal Cortex. Journal of Neurophysiology, 100(3), 1407–1419. https://doi.org/10.1152/jn.90248.2008

Mongillo, G., Barak, O., & Tsodyks, M. (2008). Synaptic Theory of Working Memory. Science, 319(5869), 1543–1546. https://doi.org/10.1126/science.1150769

Muhle-Karbe, P. S., Myers, N. E., & Stokes, M. G. (2021). A Hierarchy of Functional States in Working Memory. The Journal of Neuroscience, 41(20), 4461–4475. https://doi.org/10.1523/JNEUROSCI.3104-20.2021

Myers, N. E., Stokes, M. G., & Nobre, A. C. (2017). Prioritizing Information during Working Memory: Beyond Sustained Internal Attention. Trends in Cognitive Sciences, 21(6), 449–461. https://doi.org/10.1016/j.tics.2017.03.010

Oh, B.-I., Kim, Y.-J., & Kang, M.-S. (2019). Ensemble representations reveal distinct neural coding of visual working memory. Nature Communications, 10(1), 5665. https://doi.org/10.1038/s41467-019-13592-6

Rose, N. S., LaRocque, J. J., Riggall, A. C., Gosseries, O., Starrett, M. J., Meyering, E. E., & Postle, B. R. (2016). Reactivation of latent working memories with transcranial magnetic stimulation. Science, 354(6316), 1136–1139. https://doi.org/10.1126/science.aah7011

Spaak, E., Watanabe, K., Funahashi, S., & Stokes, M. G. (2017). Stable and Dynamic Coding for Working Memory in Primate Prefrontal Cortex. The Journal of Neuroscience, 37(27), 6503–6516. https://doi.org/10.1523/JNEUROSCI.3364-16.2017

Sprague, T. C., Ester, E. F., & Serences, J. T. (2016). Restoring Latent Visual Working Memory Representations in Human Cortex. Neuron, 91(3), 694–707. https://doi.org/10.1016/j.neuron.2016.07.006

Stokes, M. G. (2015). 'Activity-silent' working memory in prefrontal cortex: A dynamic coding framework. Trends in Cognitive Sciences, 19(7), 394–405. https://doi.org/10.1016/j.tics.2015.05.004

Stokes, M. G., Muhle-Karbe, P. S., & Myers, N. E. (2020). Theoretical distinction between functional states in working memory and their corresponding neural states. Visual Cognition, 28(5–8), 420–432. https://doi.org/10.1080/13506285.2020.1825141

Van Ede, F., Chekroud, S. R., Stokes, M. G., & Nobre, A. C. (2019). Concurrent visual and motor selection during visual working memory guided action. Nature Neuroscience, 22(3), 477–483. https://doi.org/10.1038/s41593-018-0335-6

Van Loon, A. M., Olmos-Solis, K., Fahrenfort, J. J., & Olivers, C. N. (2018). Current and future goals are represented in opposite patterns in object-selective cortex. ELife, 7, e38677. https://doi.org/10.7554/eLife.38677

Wan, Q., Cai, Y., Samaha, J., & Postle, B. R. (2020). Tracking stimulus representation across a 2-back visual working memory task. Royal Society Open Science, 7(8), 190228. https://doi.org/10.1098/rsos.190228

Wan, Q., Menendez, J. A., & Postle, B. R. (2022). Priority-based transformations of stimulus representation in visual working memory. PLOS Computational Biology, 18(6), e1009062. https://doi.org/10.1371/journal.pcbi.1009062

Wolff, M. J., Ding, J., Myers, N. E., & Stokes, M. G. (2015). Revealing hidden states in visual working memory using electroencephalography. Frontiers in Systems Neuroscience, 9. https://doi.org/10.3389/fnsys.2015.00123

Wolff, M. J., Jochim, J., Akyürek, E. G., Buschman, T. J., & Stokes, M. G. (2020). Drifting codes within a stable coding scheme for working memory. PLOS Biology, 18(3), e3000625. https://doi.org/10.1371/journal.pbio.3000625

Wolff, M. J., Jochim, J., Akyürek, E. G., & Stokes, M. G. (2017). Dynamic hidden states underlying working-memory-guided behavior. Nature Neuroscience, 20(6), 864–871. https://doi.org/10.1038/nn.4546

Wolff, M. J., Kandemir, G., Stokes, M. G., & Akyürek, E. G. (2020). Unimodal and Bimodal Access to Sensory Working Memories by Auditory and Visual Impulses. The Journal of Neuroscience, 40(3), 671–681. https://doi.org/10.1523/JNEUROSCI.1194-19.2019

Yu, Q., Teng, C., & Postle, B. R. (2020). Different states of priority recruit different neural representations in visual working memory. PLOS Biology, 18(6), e3000769. https://doi.org/10.1371/journal.pbio.3000769

Zhang, J., Ye, C., Sun, H.-J., Zhou, J., Liang, T., Li, Y., & Liu, Q. (2022). The passive state: A protective mechanism for information in working memory tasks. Journal of Experimental Psychology: Learning, Memory, and Cognition, 48(9), 1235–1248. https://doi.org/10.1037/xlm0001092

Figures

Figure 1. Two hypotheses about the underlying mechanisms of pinging the brain. During the WM maintenance, PMI and UMI were stored in different activity-silent states (PMI is easier to be reactivated) and organized by their contextual information (items were presented in different locations). Pings were task-irrelevant, high-contrast visual impulses. ***A,*** Noise-reduction hypothesis. Ping reduced the noise in the WM network and helped WM representations pop out to active state. The dotted blue lines and arrows indicated that pings indirectly reactivated the WM representations in the activity-silent state without changing their original WM processes. ***B,*** Target-interaction hypothesis. Pings interacted with PMI and UMI's representations through the overlapping locations, directly strengthening and reorganizing their neural representations. The solid red lines and arrows indicated that pings directly contacted items in the activity-silent state and changed their original storage process.

Figure 2. EEG experimental task and behavioral results. ***A,*** Experiment procedure of the delayed estimation task. Context-independent ping and context-dependent ping conditions were completed on separate days, and the recall priority was instructed before the trial. ***B,*** Recall error and response time in the two ping conditions. No differences were observed between the two ping conditions. Error bars indicated the standard error of the mean (SEM).

Figure 3. Context-dependent ping evoked more sustained and more consistent reactivations for prioritized items than context-independent ping. ***A,*** Neural representations for prioritized

items (PMI) and unprioritized items (UMI) in the context-independent and context-dependent ping conditions. The blue and red bars on the top indicated clusters with significant decoding strengths and the black bars indicated clusters with significant decoding differences between the two items ($p < 0.05$). Error shading along the decoding strength line indicated a 95% confidence interval. Gray bars on the bottom indicated the onset of the sample (S), the first ping (P1), the first recall probe (R1), the second ping (P2), and the second recall probe (R2). Transparent gray areas indicated the time window used for estimating reactivation strengths in Fig. 3*B* (-100 ms ~ 0 ms before the ping and 100 ms ~ 400 ms after the ping) The topographic maps represented the results of the searchlight analysis of the reactivation effect, and the black crosses indicated significant electrode clusters ($p < 0.05$). ***B,*** Reactivation effects for PMI after the first and second ping. During the first ping period, the first recall item was prioritized and was reactivated in both ping conditions (left darker bars); During the second ping period, the second recall item was task-relevant, and only the context-independent ping reactivated the prioritized items (right lighter bars). Error bars indicated the standard error of the mean (SEM). ***C,*** Neural decoding strengths for both items before the second ping (averaged from -100 ms to 0 ms, relative to the onset of the second ping). The left darker bars stood for decoding strengths for the first-recall item which was task-irrelevant during the second ping period; the right lighter bars stood for the second-recall item which was task-relevant during the second ping period. ***D,*** Correlations between reactivation effects after the 1st and 2nd ping in each ping condition. Each dot indicated the reactivation effect for one participant. The significant results are noted with asterisks (***: $p < 0.001$, **: $0.001 < p <= 0.01$, *: $0.01 < p <= 0.05$, †: $0.05 < p <= 0.1$).

Figure 4. Reactivations after context-dependent and context-independent pings correlated with trial-level and participant-level recall performance separately. ***A,*** Neural reactivations in the trials with smaller and larger recall errors (left) and in participants with smaller and larger recall errors (right); Error bars indicate the standard error of the mean (SEM). ***B,*** Neural reactivations in the trials with longer and shorter RTs (left) and in participants with longer and shorter RTs (right). The significant results are noted with asterisks (**: $0.001 < p <= 0.01$, *: $0.01 < p <= 0.05$).

Figure 5. Context-dependent ping stabilized the neural representations of prioritized items and changed the suppressive coding between prioritized and unprioritized items. ***A,*** Cross-time decoding results of unprioritized items (UMI, left) and prioritized items (PMI, right). The three rows indicated decoding strengths in the context-dependent and -independent ping conditions and their decoding differences. The black lines in the decoding matrix outlined clusters with significant decoding strengths or decoding differences between the two types of pings ($p < 0.05$). Gray bars on the bottom indicated the onset of the sample (S), the first ping (P1), and the first recall probe (R1). Black boxes indicated the time window of interest for further analysis in Fig. 5*B*. ***B,*** The dynamic of PMI representations after the two types of pings. The significant difference was noted with black dots ($p < 0.05$) and unfilled dots ($0.05 < p < 0.1$) on the top. ***C,*** Cross-item decoding results for PMI in the two ping conditions. The blue and red bars on the top indicated clusters with significant suppressive coding patterns ($p < 0.05$). The

transparent gray areas indicated the time window used for estimating the reactivation of suppressive coding in Fig. 5*D* (-100 ms ~ 0 ms before the ping and 100 ms ~ 400 ms after the ping). ***D,*** Reactivation effects for suppressive coding in the two ping conditions. Error bars indicated the standard error of the mean (SEM). The significant results are noted with asterisks (**: $0.001 < p <= 0.01$, *: $0.01 < p <= 0.05$).

Figure 6. Behavioral experimental task and results. ***A,*** Experiment procedure of the delayed estimation task with two retro cues, and three ping conditions were included in the task. ***B,*** Response time and recall error in the three ping conditions. Error bars indicated the standard error of the mean (SEM). The significant results of paired tests are noted with asterisks (**: $0.001 < p <= 0.01$, *: $0.01 < p <= 0.05$, †: $0.05 < p <= 0.1$).

Extended Data

Figure 3-1. No neural reactivations based on alpha power (8 ~ 12 Hz) activities among the parietal-occipital channels. Neural representations for the first recall item and second recall item across trials in the context-independent (first row) and the context-dependent ping condition (second row). The blue and red bars on the top indicated clusters with significant decoding strengths. Error shading along the decoding strength line indicated a 95% CI of the mean. Gray bars on the bottom indicated the onset of the sample (S), the first ping (P1), the first recall probe (R1), the second ping (P2), and the second recall probe (R2).

Figure 3-2. No reactivations based on voltage activities among the anterior and mid-central areas. Neural representations for PMI and UMI in the context-independent and the context-dependent ping condition. The blue and red bars on the top indicated clusters with significant decoding strengths and the black bars indicated clusters with significant decoding differences between PMI and UMI ($p < 0.05$). Error shading along the decoding strength line indicated a 95% confidence interval (CI). Gray bars on the bottom indicated the onset of the sample (S), the first ping (P1), the first recall probe (R1), the second ping (P2), and the second recall probe (R2). Transparent gray areas indicated the time window used for estimating reactivation strengths in (-100 ms ~ 0 ms before the ping and 100 ms ~ 400 ms after the ping). Error bars indicated the standard error (SEM) of reactivations.

Figure 5-1. Context-dependent ping changed the suppressive coding between PMIs and UMIs. Cross-item decoding results for PMI in the two ping conditions. The blue and red bars on the top indicated clusters with significant suppressive coding patterns ($p < 0.05$). The transparent gray areas indicated the time window used for estimating the reactivation of suppressive coding in Fig. 5*D* (-100 ms ~ 0 ms before the ping and 100 ms ~ 400 ms after the ping). Error bars indicated the standard error of the mean (SEM). The significant results are noted with asterisks. (†: $0.05 < p <= 0.1$)

Figure 1.

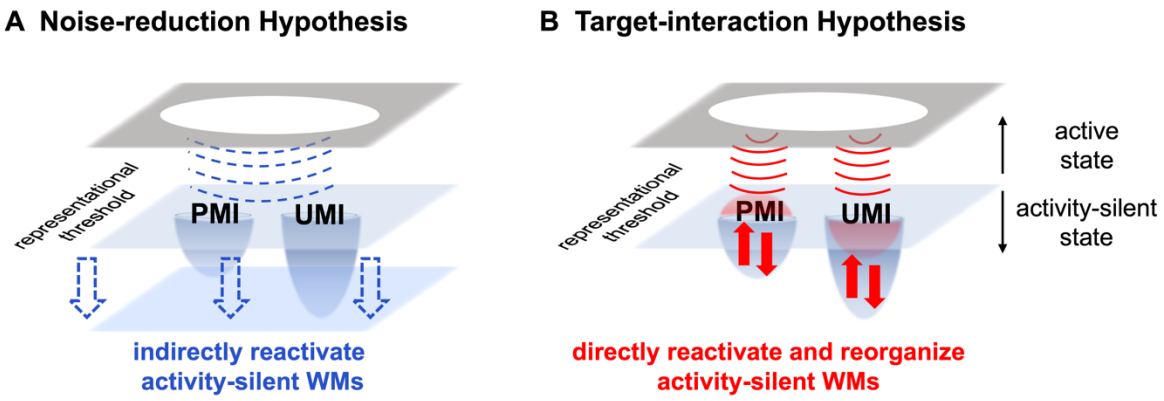
A Noise-reduction Hypothesis
representational threshold
PMI
UMI
indirectly reactivate activity-silent WMs
B Target-interaction Hypothesis
representational threshold
PMI
UMI
active state
activity-silent state
directly reactivate and reorganize activity-silent WMs

Figure 2.

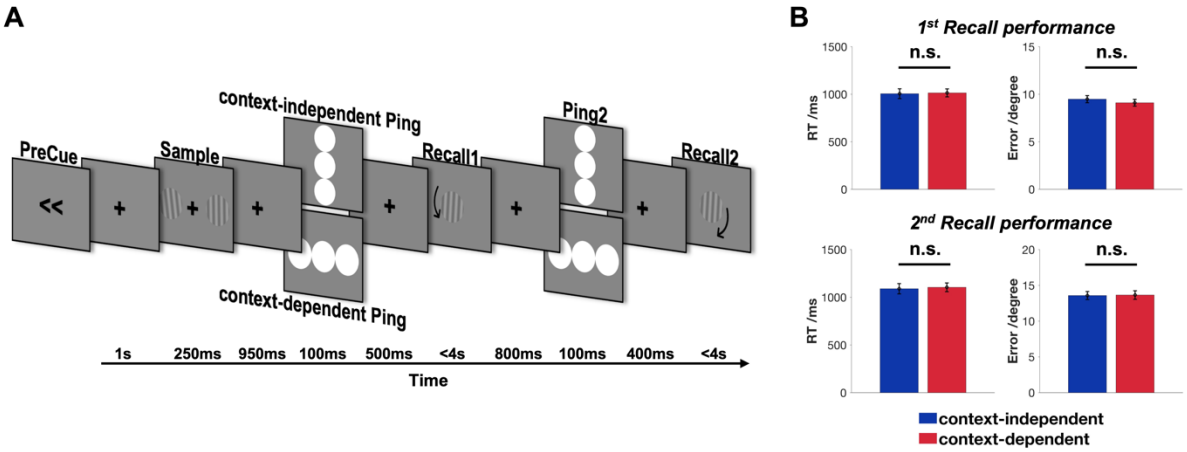
A
PreCue
Sample
context-independent Ping
context-dependent Ping
Recall1
Ping2
Recall2
<<
1s
250ms
950ms
100ms
500ms
<4s
800ms
100ms
400ms
<4s
Time
B
1st Recall performance
n.s.
n.s.
RT /ms
Error /degree
2nd Recall performance
n.s.
n.s.
RT /ms
Error /degree
context-independent
context-dependent

Figure 3.

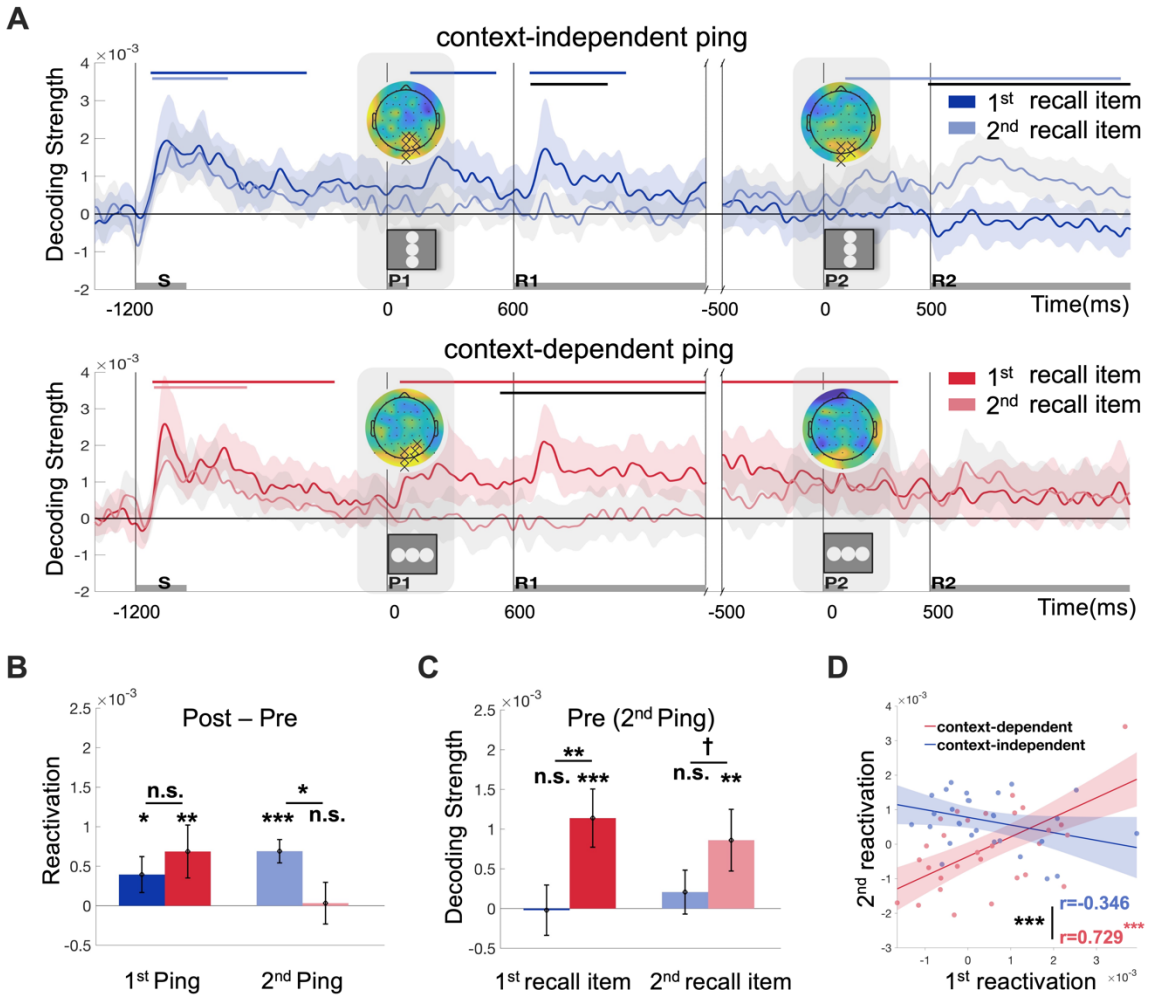
A
context-independent ping
Decoding Strength
1st recall item
2nd recall item
S
P1
R1
P2
R2
-1200
0
600
-500
0
500
Time(ms)
context-dependent ping
Decoding Strength
1st recall item
2nd recall item
S
P1
R1
P2
R2
-1200
0
600
-500
0
500
Time(ms)
B
Post – Pre
Reactivation
n.s.
*
**
*
***
n.s.
1st Ping
2nd Ping
C
Pre (2nd Ping)
Decoding Strength
**
n.s.
***
†
n.s.
**
1st recall item
2nd recall item
D
context-dependent
context-independent
2nd reactivation
r=-0.346
***
r=0.729***
1st reactivation

Figure 4.

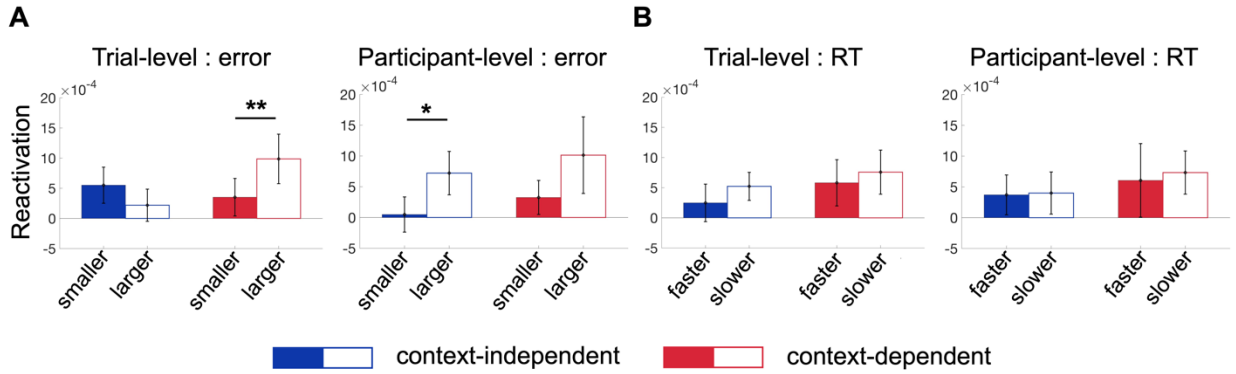
A
B
Trial-level : error
Participant-level : error
Trial-level : RT
Participant-level : RT
Reactivation
×10^-4
20
15
10
5
0
-5
**
*
smaller
larger
faster
slower
context-independent
context-dependent

Figure 5.

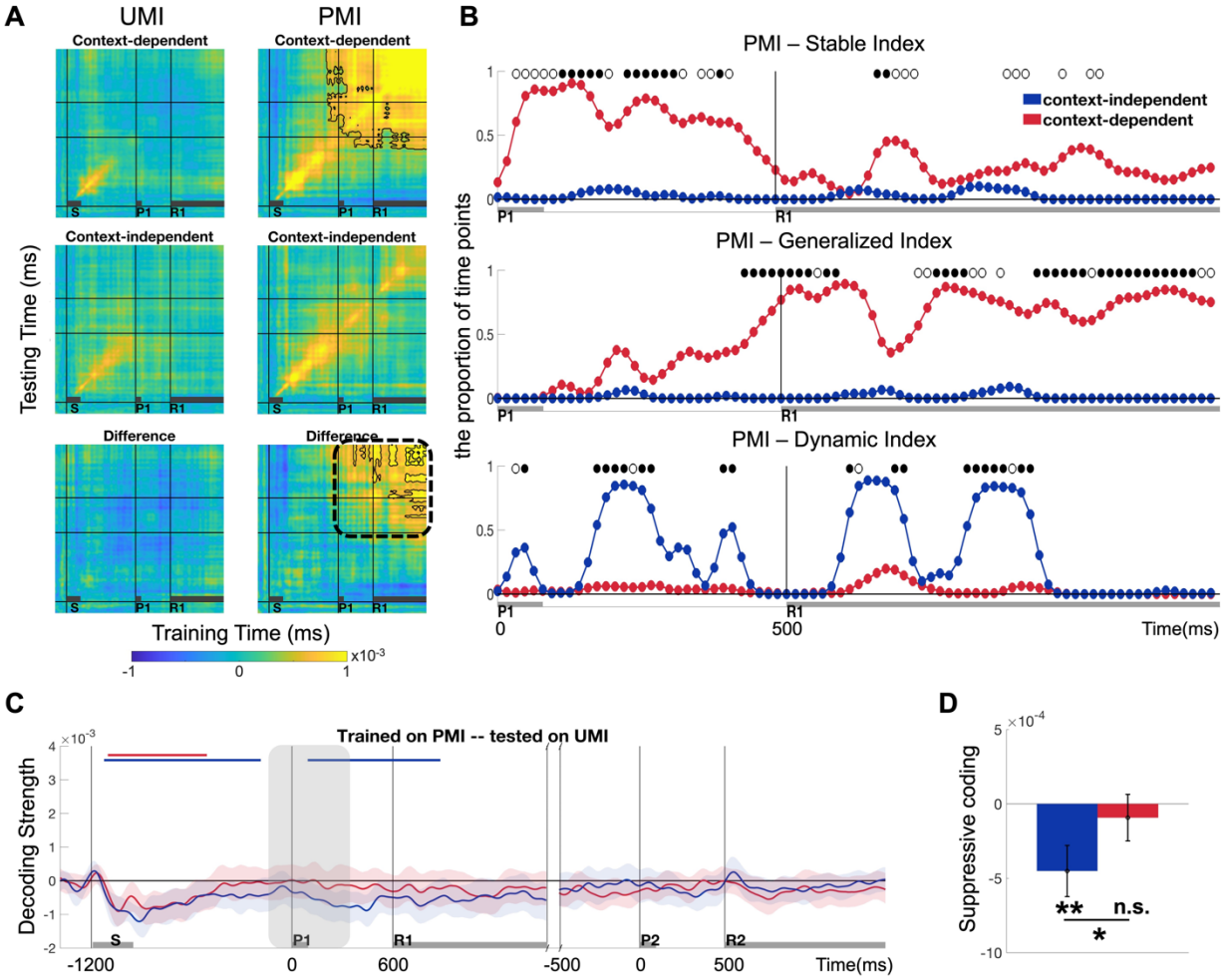
A
UMI
PMI
Context-dependent
Context-independent
Difference
Testing Time (ms)
Training Time (ms)
S
P1
R1
B
PMI – Stable Index
PMI – Generalized Index
PMI – Dynamic Index
context-independent
context-dependent
the proportion of time points
Time(ms)
C
Trained on PMI -- tested on UMI
Decoding Strength
P2
R2
D
Suppressive coding
**
n.s.
*

Figure 6.

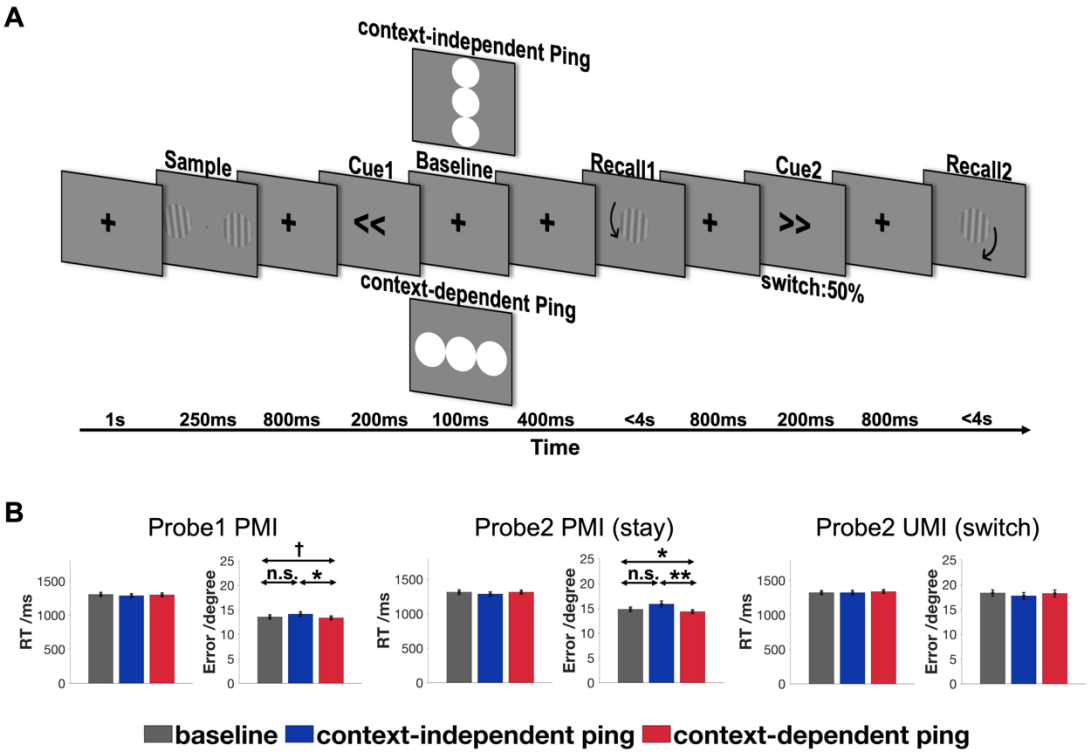
A
context-independent Ping
Sample
Cue1
Baseline
Recall1
Cue2
Recall2
<<
>>
switch:50%
context-dependent Ping
1s
250ms
800ms
200ms
100ms
400ms
<4s
800ms
200ms
800ms
<4s
Time
B
Probe1 PMI
Probe2 PMI (stay)
Probe2 UMI (switch)
RT /ms
Error /degree
n.s.
†
*
**
baseline
context-independent ping
context-dependent ping

Figure 3-1.

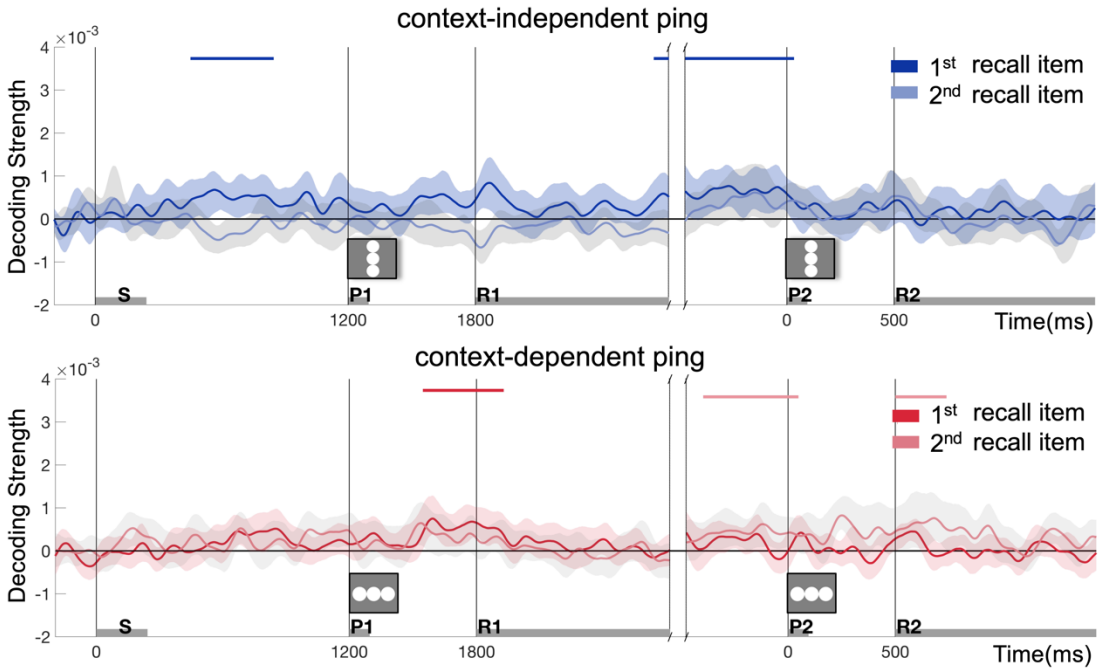
context-independent ping
Decoding Strength
×10^-3
4
3
2
1
0
-1
-2
1st recall item
2nd recall item
S
P1
R1
P2
R2
0
1200
1800
0
500
Time(ms)
context-dependent ping
Decoding Strength
×10^-3
4
3
2
1
0
-1
-2
1st recall item
2nd recall item
S
P1
R1
P2
R2
0
1200
1800
0
500
Time(ms)

Figure 3-2.

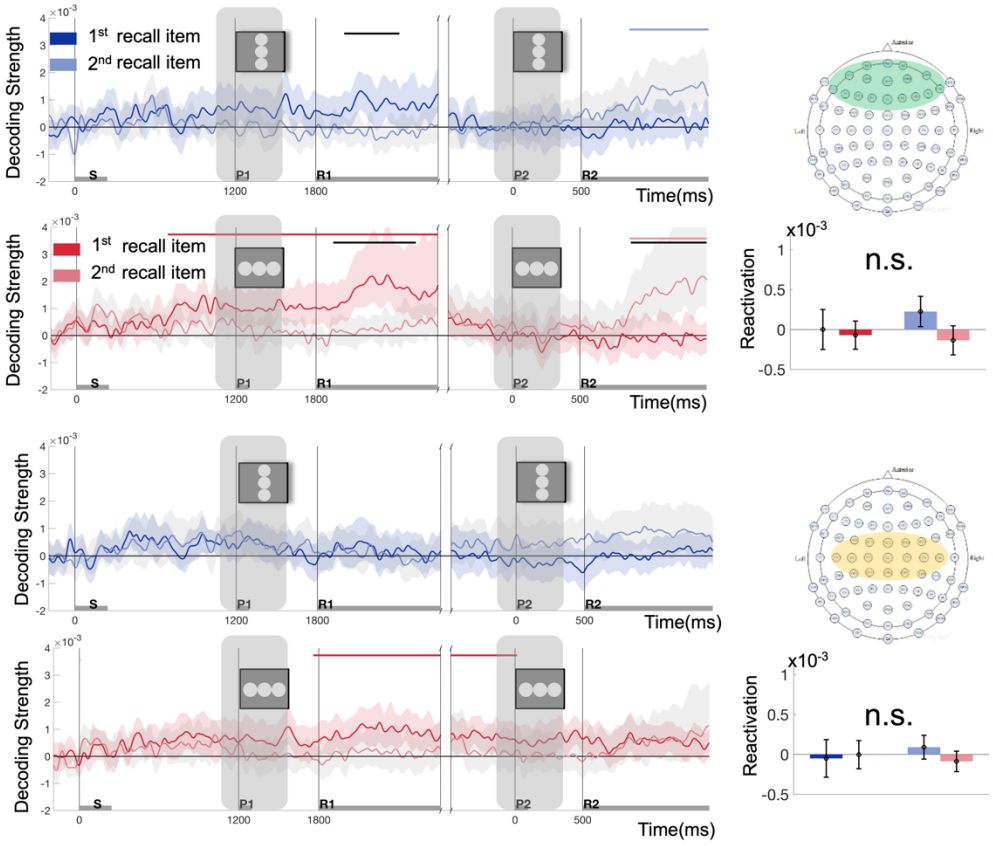
1st recall item
2nd recall item
Decoding Strength
Time(ms)
S
P1
R1
P2
R2
Reactivation
n.s.
x10-3

Figure 5-1.

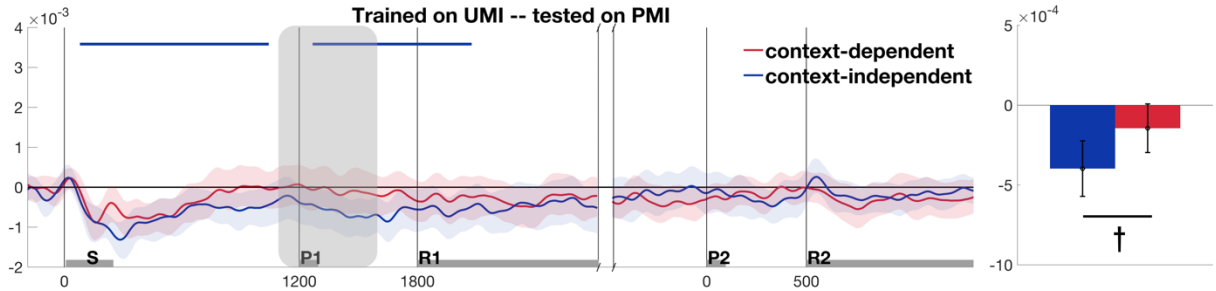
Trained on UMI -- tested on PMI
×10^-3
4
3
2
1
0
-1
-2
context-dependent
context-independent
S
P1
R1
P2
R2
0
1200
1800
0
500
×10^-4
5
0
-5
-10
†